TECHNICAL

Polymorphism of POP and SOS. I. Occurrence and Polymorphic Transformation[1]

K. Sato*[,a], T. Arishima[a], Z.H. Wang[a,2], K. Ojima[b], N. Sagi[b] and H. Mori[b]

[a]Faculty of Applied Biological Science, Hiroshima University, Higashi-Hiroshima, 724, and [b]R & D Center, Fuji Oil Co., 598, Izumisano, Japan

The polymorphic modifications of POP and SOS were identified with X-ray diffraction (XRD), DSC and Raman spectroscopy by using pure samples (99.9%). In POP, six polymorphs, α, γ, pseudo-β'_2, pseudo-β'_1, β_2 and β_1, were obtained, whereas five polymorphs, α, γ, pseudo-β', β_2 and β_1, were isolated in SOS. Thermodynamic stability increased from α to β_1 straightforwardly both in POP and SOS, because the polymorphic transformation went monotropically in the order described above. Additionally, the 99.2% sample of POP crystallized another form, δ, but the 99.9% sample did not, implying subtle influences of the impurity. The four forms, α, γ, β_2 and β_1, of POP, revealed XRD and DSC patterns identical to the four forms of SOS designated by the same symbols. The chain length structure was double in α and triple in the other three forms in both POP and SOS. Peculiarity of POP was revealed partly in the chain length structure of pseudo-β'_2 and pseudo-β'_1 which were double, whereas pseudo-β' of SOS was triple. This apparently showed contrast to the facts that the three forms revealed rather similar XRD short spacing patterns. Another peculiarity of POP was revealed in enthalpy value of the melt crystallization of α: $\Delta H_c(\alpha) = 68.1$ kJ/mol which was much larger than that of SOS (47.7 kJ/mol), and also than AOA and BOB. These peculiarities mean that the double chain length structures of POP are more stabilized than the others. Raman bands of CH_2 scissoring mode of SOS indicated parallel packing in γ, β_2 and β_1 and orthorhombic perpendicular packing in pseudo-β'. The polymorphic transformation mechanisms were discussed based on the proposed polymorphic structure models.

Polymorphism of triglycerides (TG) has been studied extensively because of its importance in oil chemistry (1) and biophysical sciences (2). The polymorphic modifications of mono-saturated acid TG have been well understood as far as the thermodynamic properties are concerned (3). As for the structural property, the crystal structures of the most stable polymorph (β) of tricaprin (4) and trilaurin (5) are determined, and the chain packing structure was discussed in detail (6,7). The structure of a metastable β' form was examined for triundecanoin using a single crystal, and compared to the structure of the β form (8). The least stable form, α, has been thought to reveal a disordered structure in which the main part of the hydrocarbon chain is oscillating around the chain axis (2,9,10).

In the literature, however, data of mixed saturated-unsaturated acid TG are still contradictory. This is manifest even in the most representative mixed acid TG, SOS (symmetric 1,3-di-steroyl-2-oleoyl glycerol). Daubert and Clarke (11) reported three forms, but soon after that Filer et al. presented two forms (12). Lutton (13) observed three forms and proposed a triple chain length structure in SOS. Malkin and Wilson showed four forms (14), but three forms were reported by Lutton and Jackson (15). Lavery (16) supported the existence of the three forms reported by Lutton and Jackson (15). In contrast, the polymorphs reported by Daubert and Clarke (11) were confirmed by Landman et al. (17). Recently, Gibon et al. presented six polymorphs of POP (symmetric 1,3-dipalmitoyl-2-oleoyl glycerol) (18). As shown below in more detail, identification of the independent polymorphic modification and the data of thermal behavior and X-ray diffraction differ from one report to another. The nomenclature is also less consistent. This discrepancy must be attributed to the samples used with different purity and also to experimental techniques. Uncertainty of this kind in the polymorphism of mixed saturated-unsaturated acids TG must be clarified, because plenty of glycerols of this kind occur in nature, and are often utilized in cocoa butter and confectionery fats (1).

The authors have recently studied the polymorphism of a series of Sat-O-Sat TG: Sat:C_{16} (POP); C_{18} (SOS); C_{20} (AOA); C_{22} (BOB) where A and B stand for arachidoyl and behenoyl acyl chains (19). Particular concern was given to isolate individual polymorphs of these compounds using X-ray diffractometry and DSC. Five polymorphs were identified and newly named: α, γ, pseudo-β', β_2 and β_1, all of which were commonly observed in the four compounds examined. Additionally another intermediate form, β', which reveals the X-ray short spacing spectra similar to β_1' of tristearin (20), was detected in POP, AOA and BOB. Because the purity of the sample in this study was rather low (up to 90%), a purer sample is needed to reduce the effect of the impurity on the polymorphism. Preliminary results of SOS using 99.0% sample were obtained recently (21), showing the same five polymorphs as previously reported (19).

This paper describes the occurrence and transformation behavior of the polymorphs in POP and SOS using the sample with purity of 99.9%. Thermal data of fusion of these forms and rates of polymorphic transformations are also presented. The polymorphic structures are discussed on the basis of X-ray diffraction spetra and Raman spectroscopic data. In a subsequent paper (II), kinetics of melt crystallization will be reported precisely.

MATERIALS AND METHODS

Initial materials of SOS for purification were prepared by solvent-recrystallization of cocoa butter using n-hexane. POP was synthesized through enzymatic esterification using triolein and ethyl palmitate. A sample approximately 99% pure was first obtained by a preparative HPLC (Killoprep 250, Millipore Co. Ltd.). For comparison to polymorphic behavior in the 99.9% sample, we examined the 99.2% sample of POP and 99.0% of SOS, whose glyceride compositions are as follows; POP (99.2%):

[1]Presented at the AOCS annual meetings in New Orleans, Louisiana in May 1987 and Phoenix, Arizona in May 1988.

*To whom correspondence should be addressed.

[2]Present address: Hei Long Jiang Commercial College, People's Republic of China.

POS (0.2%), SOS (0.1%), POO (0.2%), PLS (L; linoleic, 0.2%), diglycerides (0.1%), and SOS (99.0%): POP (0.1%), POS (0.3%), PPS (0.3%), SSS (0.2%), diglycerides (0.1%). The 99.9% samples of POP and SOS were produced with the same HPLC using the initial material of 99% purity. The purity of the final sample was determined by HPLC (Japan Spectroscopic Co. Ltd.) under the following conditions: column, Lichrosorb RP-18 (Merck), 5 μm, 4.6ϕ × 25 cm, A-303 ODS (Yamamura Chemical Lab.), 5 μm, 4.6 ϕ × 25 cm; solvent, acetone/acetonitrile, 80:20 (volume ratio); sample conc. 4% (w/v) acetone solution, 20 μl; carrier velocity, 1.0 ml/min; temperature, 20°C; detector, refractive index detector; sensitivity, range 1, and attenuation, 256. The impurity in the 99.9% sample of POP and SOS was not identified.

The occurrence of polymorphs was examined by two modes of crystallization. The first one was simple cooling of the melt from 80°C to varying crystallization temperatures (T_c). The second was done via melt-mediated transformation (22), e.g., more stable forms were crystallized after the melting of less stable forms by rapidly raising the temperature. This method provides additional data to those examined by the simple melt cooling. In each crystallization procedure, the temperature of a growth cell was rapidly changed by switching the circulating water connected to two thermostats.

The polymorphic transformation was induced by tempering the sample which was put on the glass plate used for X-ray diffraction (XRD), (Rigaku, Cu-K_α). Small angle XRD was carried out on the transformation from γ to pseudo-β_2' of POP (Rigaku, CuK_α, 60 kV, 200 mA, slit angles 0.04° and 0.03°, 2 θ scan from 0.1° to 5.0°). The polymorphic transformation was induced at different tempering temperatures (T_t: 0.1°C), being examined by the XRD pattern and the melting peak of Differential Scanning Calorimetry (DSC: Rigaku DSC-8230). The two data were always taken for the same sample simultaneously by the following procedure; the sample utilized for DSC (1.5 ∼ 1.7 mg) was picked off from the powder sample utilized for XRD (∼100 mg), and measured at the same time as the XRD scan. The polymorphic transformation was examined three times in every case. The room temperature where the XRD and DSC studies were carried out was kept at 12°C. The transformation during the XRD scan was actually hindered at this temperature.

Isolation of an independent polymorph was justified only when the sample exhibited reproducible unique data of the single melting peak and the XRD long and short spacing patterns. In some samples, it happened that different melting and long spacing peaks superimposed even when the XRD short spacing pattern was apparently unique. In this case, further tempering was applied to get the best commensuration among the three data. It was still difficult, however, to obtain the single long spacing peak, particularly in the metastable forms of POP, although the DSC melting and XRD short spacing revealed the single pattern. This feature may imply a peculiarity of the polymorphism of POP. The heating rates of DSC were 1, 2 or 5°C/min, while the cooling rate was 2°C/min. The melting point was defined, by computerized data-processing, as a crossing point between the base line and the tangential line of a maximal slope of the initial endothermic peak. The temperature of the peak-top position was higher than the above defined melting point by 1.5 ∼ 2°C. With increasing heating rate from 1°C/min to 5°C/min, the peak temperature of melting was increased by ∼ 2°C. The above-defined melting point, however, did not depend largely on the heating rate. The single melting peak was available for each modification even at the heating rate of 1°C/min, except for α, whose melting was always accompanied by rapid crystallization of γ.

RESULTS

X-ray diffraction. XRD short spacing patterns of seven polymorphs of POP and five polymorphs of SOS are shown in Figure 1. Table 1 summarizes the d-values and relative intensities of the XRD short spacing spectra of POP and SOS. It must be noted that there was no significant difference in the XRD patterns for each polymorph taken at 12°C and just below its melting point. This means that the crystalline packing is uniquely determined in each polymorph.

The diffraction patterns of α, γ, β_2 and β_1 of POP are essentially the same as those of SOS. α has a single peak at 4.21 A. Characteristic of γ are two strong peaks at 4.74 A and 3.90 A in POP and 4.72 A and 3.88 A in SOS. β_2 and β_1 have a strong peak at 4.58 A in SOS and 4.61 A in POP. Main differences between β_2 and β_1 appear in intermediate peaks of 4 ∼ 3.5 A both in POP and SOS. In SOS, two peaks of β_2 denoted by arrows (4.00 and 3.90 A) are split into two in β_1, and weak peaks in β_2 denoted by filled triangles (3.75 and 3.57 A) disappeared in β_1. A peak of 3.65 A is much stronger than the other four peaks of β_1. In POP, the peaks at 3.93, 3.55 and 3.52 A of β_2 became weak, whereas the peaks at 3.72 A and 3.67 A became stronger in β_1 (Table 1).

Besides the above four polymorphs, the XRD short spacing patterns of pseudo-β′ of SOS, and, δ, pseudo-β_2' and pseudo-β_1' of POP differ from each other in a subtle but distinctive manner. Pseudo-β′ of SOS exhibits two strong peaks at 4.02 and 3.70 A and four weak peaks. No strong peak appears at 4.72 A or at 4.58 A. In the case of POP, three forms of δ, pseudo-β_2' and pseudo-β_1' are similar to pseudo-β′ of SOS, yet clear differences are detectable. Pseudo-β_2' and pseudo-β_1' have two strong peaks at 4.23 A and 3.96 A, and at 4.27 A and 3.96 A, respectively. Delta reveals three strong peaks at 4.29, 4.13 and 3.83 A. More convincing differences between the three forms are seen in the DSC melting peak and in the XRD long spacing as described below.

Figure 2 shows characteristic XRD long spacing spectra of (a) α and γ of SOS; (b) γ and pseudo-β_2', and (c) pseudo-β_2' and β_2 of POP. Figure (b) is the small angle XRD pattern. All of these patterns are taken during the transformation processes. Every spectrum is labeled with (00l) indices which correspond to the interlamellar distances (Table 1). The β_2 and β_1 forms have the same long spacing values both in POP and SOS. The pseudo-β_2' and pseudo-β_1' forms of POP have the same long spacing. The chain length structure (13, 23) was considered by taking into account the length of glycerol bone, and stearic and palmitic lamellae. In SOS, α is double chain length and the other four forms are triple chain length. In POP, the double chain length structure is revealed in α, and γ, δ, β_2 and β_1 are triple chain length. As for the long spacing value of pseudo-β_2' and pseudo-β_1' of POP,

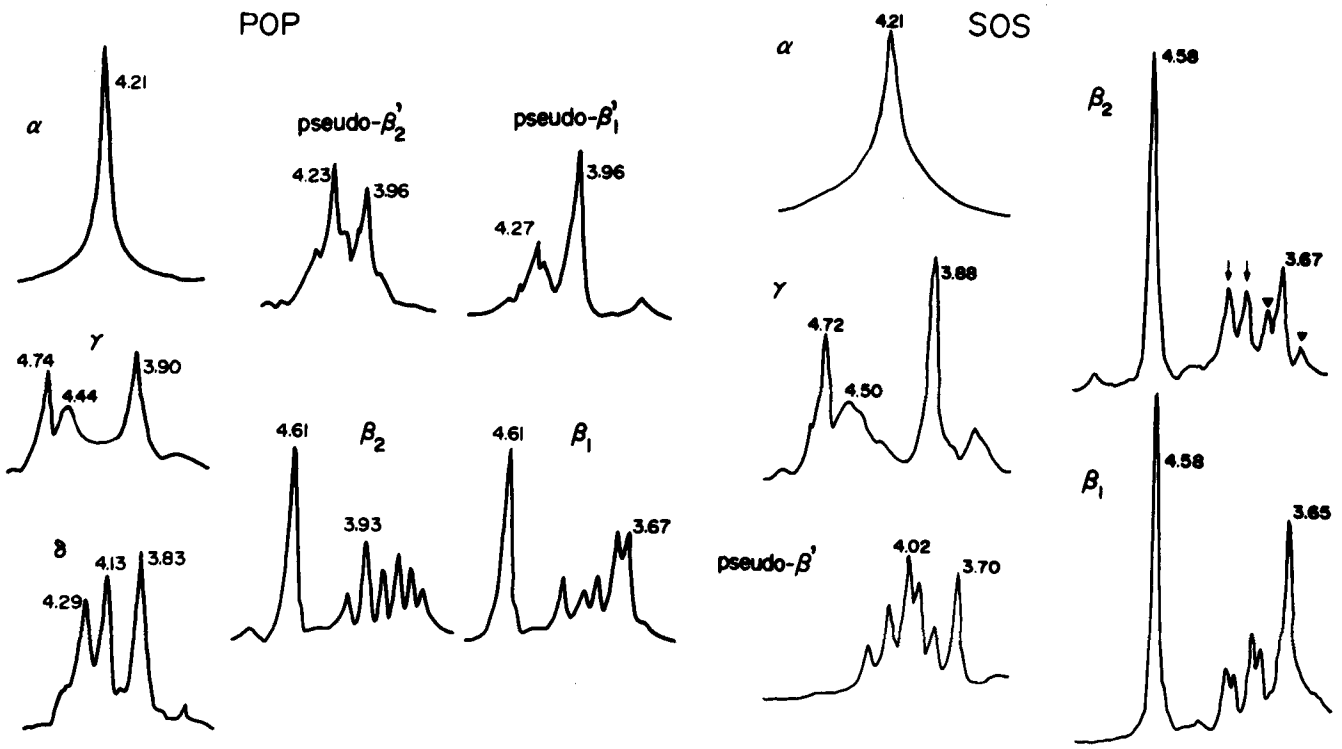

FIG. 1. X-ray diffraction spectra of short spacing of the polymorphs of POP and SOS.

TABLE 1

X-ray Diffraction Long Spacing and Short Spacing of Polymorphs of POP and SOS

	Long spacing (A)	Short spacing (A)							
POP									
α	46.5	4.21 (vs)							
γ	65.4	4.74 (s)	4.46 (m)	3.90 (s)	3.58 (w)				
δ	62.5	4.29 (s)	4.13 (s)	3.83 (s)					
pseudo-β'_2	42.4	4.38 (w)	4.23 (s)	4.15 (m)	3.96 (s)	3.83 (w)			
pseudo-β'_1	42.4	4.45 (w)	4.27 (m)	4.13 (m)	3.96 (s)				
β_2	61.0	4.61 (vs)	4.07 (m)	3.93 (m)	3.82 (m)	3.72 (m)	3.62 (w)	3.55 (w)	3.52 (w)
β_1	61.0	4.61 (vs)	4.07 (m)	3.88 (m)	3.82 (m)	3.72 (s)	3.67 (m)		
SOS									
α	48.3	4.21 (vs)							
γ	70.5	4.72 (s)	4.50 (m)	3.88 (s)	3.63 (w)				
pseudo-β"	70.0	4.30 (m)	4.15 (m)	4.02 (s)	3.95 (m)	3.83 (m)	3.70 (s)		
β_2	65.0	4.58 (vs)	4.00 (m)	3.90 (m)	3.75 (m)	3.67 (m)	3.57 (w)		
β_1	65.0	4.58 (vs)	4.02 (w)	3.97 (w)	3.85 (w)	3.80 (w)	3.65 (s)		

42.4 A, three chain length structures are considered, double, quadruple and sextuple. The quadruple layer, 84.8 A, or sextuple layer, 127.2 A, must show (001) long spacing peaks at diffraction angles 2θ of 1.05° or 0.7°, respectively. However, the XRD pattern of the sample undergoing the $\gamma \rightarrow$ pseudo-β_2' transition showed no peak at $2\theta = 0.1 \sim 2.0°$ except the (002) peak of the triple-chain-length γ form of 65.4 A (Fig. 2b). Hence, we conclude that the long spacing value of 42.4 A corresponds to the double chain length structure.

Occurrence. All polymorphs except for β_1 were crystallized and isolated from either melt cooling or melt mediation. The details of the melt crystallization will be reported in paper II. α occurred by chilling the melt below its melting point. The melt cooling and melt mediation produced γ, pseudo-β' of SOS, and γ, pseudo-β_2', and pseudo-β_1' of POP. The γ-melt mediation induced the occurrence of pseudo-β' and β_2 of SOS, and pseudo-β_2', pseudo-β_1' and β_2 of SOS, and pseudo-β_2', pseudo-β_1' and β_2 of POP. The δ form of POP was obtained only from 99.2% by the melt cooling method in a range of T_c between 25 and 26.5°C. However, this form did not occur in the 99.9% sample.

DSC data. The present DSC thermograms did not

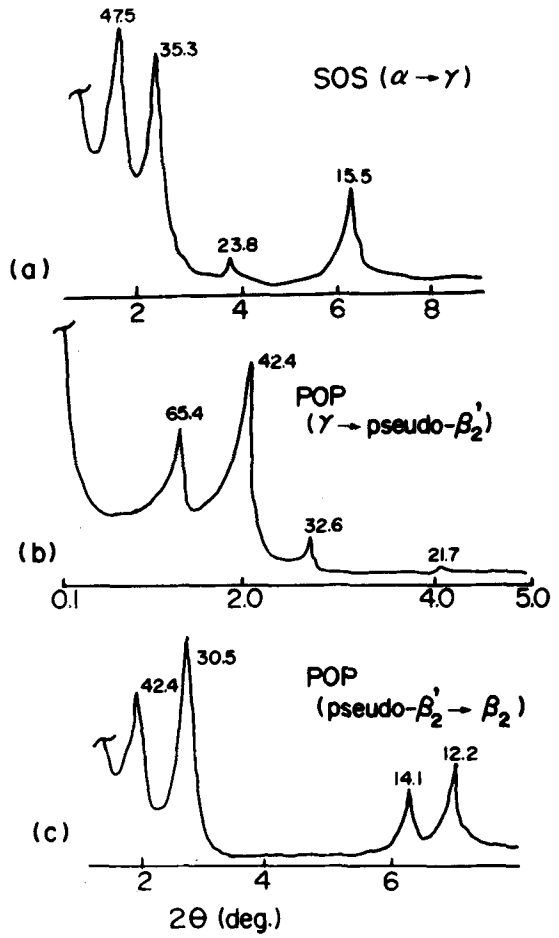

FIG. 2. X-ray diffraction spectra of long spacing of the polymorphs of POP and SOS. (a) α and γ of SOS; (b) γ and pseudo-β'_2 of POP, and (c) pseudo-β'_2 and β_2 of POP (Table 1). Small angle XRD peaks are shown in (b).

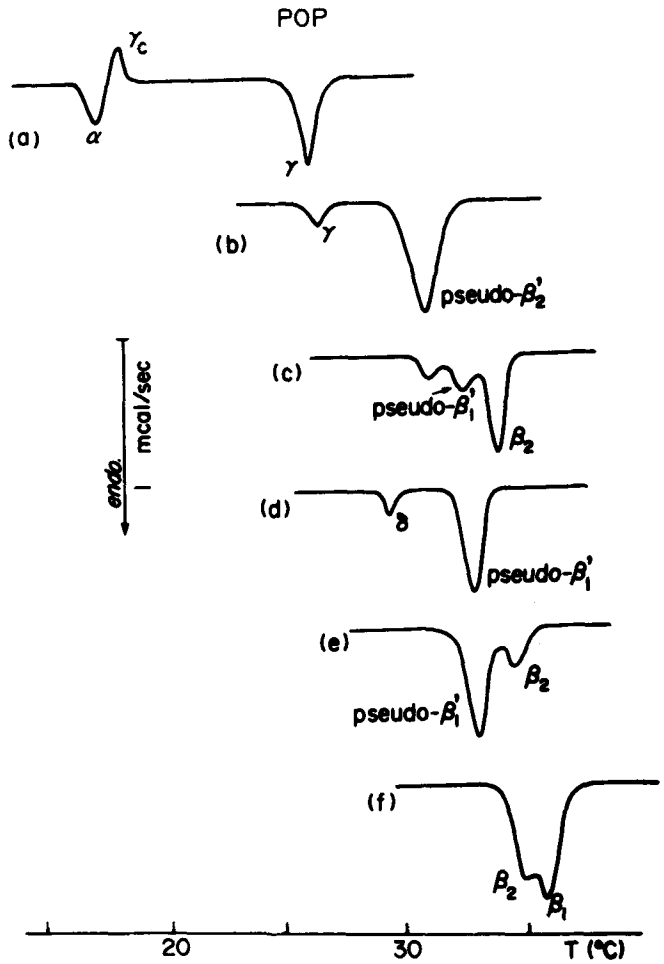

FIG. 3. DSC melting peaks of the polymorphs of POP at a heating rate of 1°C/min. In (a), the melting of α is followed by rapid crystallization of γ which then melts at 27.0°C. In (b) through (f), all endothermic peaks mean the melting of independent polymorphs which existed concurrently in the thermally-treated samples, not revealing exothermic polymorphic transitions during the heating process. Melting of (b), γ and pseudo-β'_2; (c) pseudo-β'_2, pseudo-β'_1 and β_2; (d) δ and pseudo-β'_1; (e) pseudo-β'_1 and β_2, and (f) β_2 and β_1.

exhibit exothermic peaks of the polymorphic transformations which may occur during the heating process except for α, even at a heating rate of 1°C/min. In the case of α both in POP and SOS, the fusion of α was always followed by crystallization of γ. The DSC melting patterns of SOS were reported previously (19). Figure 3 displays the melting peaks of the POP samples revealing multiple polymorphs, which were made by the tempering procedures.

The fusion of α at 15.2°C was soon followed by crystallization of γ which melts at 27°C (Fig. 3a). The other six polymorphs revealed isolated melting peaks as shown in Figure 3b–3f, all of which were taken for the samples undergoing polymorphic transformations. A general tendency was that, during successive transformations from α to β_1, the higher-melting peak increased in size at the expense of the lower-melting peak with increasing tempering duration. Among the six transformations, the conversion through pseudo-β_2' or pseudo-β_1' was curious.

The γ form completely transformed to pseudo-β_2'. Thereafter, pseudo-β_2' transformed both to pseudo-β_1' and β_2, regardless of the mode of occurrence of the pseudo-β_2' form, melt cooling, α-melt or γ-melt mediation, as shown in Figure 3c. The melting peak of pseudo-β_1' still appeared after pseudo-β_2' disappeared, always being smaller in size than that of β_2. Further tempering caused an increase in the β_2 melting peak at the expense of pseudo-β_1'. In contrast, the δ form converted directly to pseudo-β_1', not through pseudo-β_2' which subsequently transformed to β_2, as exhibited in Figure 3d and 3e. Finally, the β_2 form converted to β_1, as shown in separate DSC melting peaks in Figure 3f.

Consequently, the melting point (T_m) and enthalpy (ΔH_f) of fusion of all polymorphs using the samples of 99.9% purity are displayed in Table 2. The data of crystallization were taken for α, because no single melting peak was available. As for SOS, we confirmed that there was no appreciable difference between the samples of 99.0% (21) and 99.9% (present) within the experimental errors. As for α, the values of crystallization (ΔH_c) are shown, because the data for fusion cannot be obtained directly. One may reasonably anticipate that the polymorph of higher melting point may have larger values of T_m and ΔH_f, because the polymorphism is monotropic.

TABLE 2

Thermal Data of SOS and POP Polymorphs

	T_m (°C)	ΔH_f[a] (KJ/mol)
SOS		
α	23.5	47.7[b]
γ	35.4	98.5
pseudo-β'	36.5	104.8
β_2	41.0	143.0
β_1	43.0	151.0
POP		
α	15.2	68.1[b]
γ	27.0	92.5
δ	29.2	107.5
pseudo-β_2'	30.3	95.5
pseudo-β_1'	33.5	98.3
β_2	35.1	124.4
β_1	36.7	130.2

[a]Experimental errors: T_m, ±1°C for α and ±0.3°C for others; ΔH_f, ±7 KJ/mol for β_2 and β_1 in SOS and POP, ±3 KJ/mol for others.
[b]Enthalpy of melt crystallization was measured on α.

This applies to all polymorphs of SOS and POP except for δ. T_m of δ is 29.2°C, which is lower than those of pseudo-β_2' and pseudo-β_1' by 1.1°C and 4.3°C, respectively. However, ΔH_f of δ is larger than those of pseudo-β_2' and pseudo-β_1'. For example, the difference in ΔH_f between δ and pseudo-β_2 is 12 KJ/mol, which is approximately four times as large as the difference between γ and pseudo-β_2' (3 KJ/mol). This peculiarity is characteristic of POP, and is also exhibited in the transformation feature described below.

Transformation rates. All transformations of POP and SOS were irreversible, implying the monotropic nature of the polymorphism. The transformation behavior was examined precisely at different temperatures using as indicators the XRD short and long spacings and the DSC melting peak. It is worthy to note that the initiation and completion of the transformation were reflected on the above three indicators in different manners. This means the importance of examining the transformation processes with multiple techniques.

Table 3 summarizes the transformation rate, which was defined as a duration during which the single melting peak of the initial polymorph completely converted into the single melting peak of the next stable form at a constant temperature in the DSC patterns. An average of three trials is shown for each transformation. There was one transformation pathway in SOS; $\alpha \rightarrow \gamma \rightarrow$ pseudo-$\beta' \rightarrow \beta_2 \rightarrow \beta_1$. In contrast, POP exhibited two pathways; $\alpha \rightarrow \gamma \rightarrow$ pseudo-$\beta_2' (\rightarrow$ pseudo-$\beta_1') \rightarrow \beta_2 \rightarrow \beta_1$ in the 99.9% sample, and $\delta \rightarrow$ pseudo-$\beta_1' \rightarrow \beta_2 \rightarrow \beta_1$ in the 99.2% sample. The transformation rate from pseudo-β_2' to pseuso-β_1' is not shown, because the separation of the two peaks was not successful. It appears that, in all pathways, the transformation needed higher thermal energy and took longer duration as the polymorph approached the most stable from, β_1. Particularly, the $\beta_2 \rightarrow \beta_1$ transformation was significantly delayed.

TABLE 3

Rate of Polymorphic Transformation of SOS and POP in a Solid State

SOS	$\alpha \rightarrow \gamma$	$\gamma \rightarrow$ pseudo-β'	pseudo-$\beta' \rightarrow \beta_2$	$\beta_2 \rightarrow \beta_1$
	12 hr (15°C)	1.5 hr (35°C)	8 hr (35°C)	2.5 days (40°C)
POP	$\alpha \rightarrow \gamma$	$\gamma \rightarrow$ pseudo-β_2'	pseudo-$\beta_2' \rightarrow \beta_2$	
	1 hr (12°C)	2.5 hr (25°C)	36 hr (30°C)	$\beta_2 \rightarrow \beta_1$
		$\delta \rightarrow$ pseudo-β_1'	pseudo-$\beta_1' \rightarrow \beta_2$	14 days (30°C)
		10 hr (26.5°C)	40 hr (30°C)	

The changes in the XRD long spacing in five typical transformations are shown in Figure 4, being described by $I_2/(I_2 + I_3)$ in which I_2 and I_3 are the intensities of the long spacing for double-chain length and triple-chain length, respectively. Each transformation took place at the same temperature as that displayed in Table 3. In SOS, there was no appreciable difference between DSC and the long spacing concerning the cessation of transformation. In POP, however, the conversion in long spacing was delayed during some transformations, most remarkably, in pseudo-$\beta_2' \rightarrow \beta_2 \rightarrow \beta_1$ at 30°C: 36 hr with DSC, while ca. 25 days with the long spacing. Similar delay was observed in $\gamma \rightarrow$ pseudo-β'_2. In the case of $\alpha \rightarrow \gamma$, the long spacing changed fastest, yet, in turn, the rate of decrease of $I_2(\alpha)$ was slower. The XRD long spacing of pseudo-β_2' appeared before the conversion from α to γ was complete.

Table 4 summarizes the initiation and completion of all the transformations in POP and SOS, indicated by the three parameters. In SOS, the change in the XRD short and long spacings simultaneously initiated in the transformation of $\alpha \rightarrow \gamma$. Meanwhile, in $\gamma \rightarrow$ pseudo-$\beta' \rightarrow \beta_2$, the short spacing changed faster than the long spacing and DSC, which changed synchronously. In $\beta_2 \rightarrow \beta_1$, the short spacing first changed, but the cessation in the XRD short spacing and DSC occurred simultaneously. POP revealed rather complicated features. As for the onset of transformation, the long spacing was first indicative for $\alpha \rightarrow \gamma$, but long and short spacings changed more or less synchronously in the other transformations. As for the cessation of transformation, the short spacing and DSC were completed at the same time in $\beta_2 \rightarrow \beta_1$. In other cases, the long spacing was delayed, or DSC and long spacing followed the short spacing.

The nonsynchronous transformation behavior described here may mean a certain peculiar nature which characterizes the transformation process itself, although sensitivity of the experimental techniques like DSC melting also may account for some tendency.

DISCUSSION

In this study, the polymorphism of POP and SOS exhibited complicated behavior. Accordingly, we gave rather complicated nomenclature to the polymorphs which differ greatly from those reported in previous studies. Therefore, we first discuss the number of independent polymorphs and the nomenclature. Thereafter, the crystal structure, in particular the chain length structure

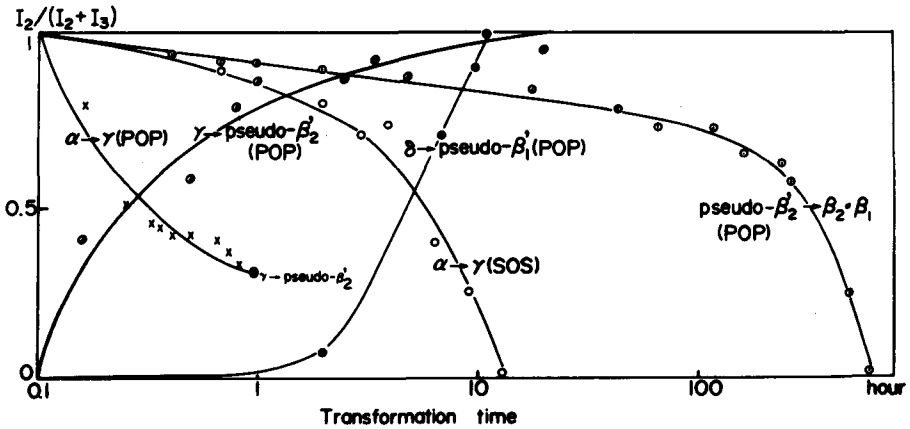

FIG. 4. Changes in intensity ratio of X-ray diffraction long spacing spectra of double (I_2) and triple (I_3) chain-length structures during five typical polymorphic transformations of POP and SOS.

TABLE 4

Order of Changes in XRD Short Spacing (S), Long Spacing (L) and DSC Melting (D) during Polymorphic Transformations of POP and SOS[a]

Transformation	T_t (°C)	Initiation	Completion
SOS			
$\alpha \rightarrow \gamma$	15	S ~ L	S > D ~ L
$\gamma \rightarrow$ pseudo-β'	35	S	S > D ~ L
pseudo-$\beta' \rightarrow \beta_2$	35	S	S > D ~ L
$\beta_2 \rightarrow \beta_1$[b]	40	S	S ~ D
POP			
$\alpha \rightarrow \gamma$	12	L	S > D[c]
$\gamma \rightarrow$ pseudo-β_2'	25	S ~ L	S > D > L
pseudo-$\beta_2' \rightarrow \beta_2$	30	S ~	S > D > L
$\beta_2 \rightarrow \beta_1$[b]	30	S	S ~ D
$\delta \rightarrow$ pseudo-β_1'	26.5	S ~ L	S > D ~ L
pseudo-$\beta_1' \rightarrow \beta_2$	30	S ~ L	S > D > L
$\beta_2 \rightarrow \beta_1$[b]	30	S	S ~ D

[a] Changes at initiation and completion of the transformation are measured separately.

[b] β_2 and β_1 have the same long spacing.

[c] Long spacing peak of α was superposed with that of pseudo-β_2' before complete disappearance of α.

and the subcell packing, thermal behavior and the mechanism of polymorphic transformation will be discussed.

Independent polymorphs and nomenclature. In the nomenclature of the polymorphism of glycerides, Larsson's method (24) has been used, based primarily on the subcell packing: α having the hexagonal packing (H), β' orthorhombic perpendicular packing (O⊥) and β-triclinic parallel ($T_{//}$). Subscripts, such as β'_1 or β'_2, were given to multiple modifications having the same subcell structure, a subscript 1 standing for the more stable form. In the literature of Sat-O-Sat triglycerides, the nomenclature used in earlier data was similar to Larsson's (24), but recent studies tried to use different names (25). This may be because complexity in the polymorphism of the Sat-O-Sat TG might not fit the nomenclature of the mono-saturated acid TG in a straightforward manner. For example, all polymorphs of the mono-acid triglycerides are stacked according to the double chain length, whereas the thermodynamically stable polymorphs of SOS and POP exhibit the triple chain length in which the saturated and oleic acyl chains are segregated. The possibility arises that the subcells of the two lamella are different, as discussed on SOS (23). Therefore, the nomenclature simply based on the subcell structure does not apply to the present case.

Our nomenclature is based both on Larsson's method and on structural characteristics which were newly found in the present study (Table 5). A comparison with earlier reports was based primarily on the XRD short spacing, not on the melting point, such as Landmann et al. (17). This is because the difference in the purity of the sample may not alter the subcell packing substantially, whereas it changes the melting behavior remarkably. Besides Table 5, sub-α, α and β of SOS were observed, but no precise data were presented (25).

The α form was the same as those in all reports except form 5 of Lovegren et al. on POP (26). α first crystallizes by chilling the melt, exhibiting single XRD short spacing peak.

γ is a new polymorph in this study. The major characteristics of γ are as follows; more stable than α but still metastable, triple chain length, a strong XRD short spacing peak around 4.7 A, and parallel subcell packing. There is no corresponding form in the mono-saturated acid TG. As a reference, we may note that γ of oleic acid has a strong short spacing at 4.71 A characteristic of the $O'_{//}$ packing (27). Therefore, the name γ was selected. β' (12), β'' (14,16) or sub-β (15,16) may also be inadequate because they have some similarity to β' or β of mono acid TG, respectively. In POP, two forms, 3 and 4 (26), or L_2 and L_3 which indicate a liquid crystalline structure (18), correspond to γ. The polymorphic transformations (Table 3), either from α to γ or from γ to pseudo-β', might be considered the occurrence of the two forms.

As for δ in POP, it occurred in the 99.2% sample but not in 99.9%. Thus, δ is not an independent polymorph of POP, but occurred most probably due to an impurity effect. Interestingly, two reports presented the same

TABLE 5

Nomenclature of the Polymorphs of POP and SOS

POP							SOS					
Present	α	γ	δ[a]	pseudo-β_2'/pseudo-β_1'	β_2/β_1	Ref.	Present	α	γ	pseudo-β'	β_2/β_1	Ref.
Filer et al.	—	—	—	β'	β	12	Filer et al.	—	β'	β'	β	12
Malkin and Wilson	α	β''	—	β'	β	14	Lutton	α-3	X-3	—	β-3	13
Lutton and Jackson	α-2	—	sub-β'-2	β'-2	β-3	15	Malkin and Wilson	α	β''	β'	β	14
Lavery	α-2	β''	—	β'-2	β-3	16	Lutton and Jackson	α-3	sub-β-3	β'-3	β-3	15
Lovegren et al.	5	4,3	—	2	1	26	Lavery	α-3	sub-β-3	—	β-3	16
Gibon et al.	α-2	L_2,L_3	sub-β'-2	pseudo-β'-2	β-3	18						

[a]δ was observed in 99.2% sample, not in 99.9% sample.

XRD short spacing patterns as δ, being called sub β'-2 (15,18).

Pseudo-β' in SOS and pseudo-β'_2 and pseudo-β'_1 in POP were named based on the nomenclature of Gibon et al. (18), all revealing similar XRD short spacings. Use of β' means an existence of the $O_\perp$ packing in SOS as revealed in Raman scattering data. "Pseudo-" means a certain deviation from the ordinary β' form of the mono-saturated acid TG. Subscripts in two pseudo-β' forms of POP were given so that the higher melting form has a subscript 1.

β_2 and β_1 were based on the XRD short spacings similar to β of mono-saturated acid TG, with increasing subscripts denoting decreasing melting point. Differentiation of β_2 and β_1 in POP and SOS was done in this study for the first time.

In our two earlier reports, the purity of sample was comparatively low, 91.3% (19) and 99.0% (21) for SOS and 90.4% (19) for POP. SOS exhibited the same five independent polymorphs in the three different samples. However, the polymorphs of POP differed except for the four forms of α, γ, β_2 and β_1; namely, β' and pseudo-β' (90.4%) (19) and δ, pseudo-β'_2 and pseudo-β'_1 (99.2%), and pseudo-β'_2 and pseudo-β'_1 (99.9%) in the prsent study. We think the 99.9% sample must reveal the intrinsic polymorphism of POP.

Finally, some previous reports used another subscript to indicate the chain length structure, for example, β-3 (13,16,18) for the triple chain length. We did not use it, which may result in confused nomenclature.

Chain length structure. The chain length structure of complicated TG depends on the difference in the acyl chain structure. In the saturated acid TG, difference in the number of carbon atoms of the acyl chains is most determinative (28). In the mixed saturated-unsaturated acid TGs, both the double and triple chain length structures were observed in the past, but precise examination on the conversion of the chain length structure during a given set of polymorphic transformations has been lacking.

In SOS, the long spacing of α is 47.5 A. This value lies between tristearin α: 50.6 A (29) and triolein α: 44.8 A (30), both of which are of double chain length. Therefore, SOS α is of double chain length. Some earlier studies, however, reported that α is triple, because of the long spacing values of 80.5 A (13) or 80.6 A (16). It is highly possible that the diffraction indices of the long spacing spectra might be confused in these studies, e.g., 16.3 A was read $d_{(005)}$ (13), but it must be $d_{(003)}$. Malkin and Wilson (14) reported the double chain length of α. All the polymorphs of SOS except α are triple, in accordance with the earlier work. The long spacing values decreased in increasing order of the thermodynamic stability, β_2 and β_1 having the same long spacing. It is worthy to note here that α shows an intensity relation of the XRD long spacing peaks with three smaller indices like $I{:}d_{(001)} > I{:}d_{(003)} > I{:}d_{(002)}$. This relation holds in the crystals of double chain length in fatty acids and mono-acid TGs. On the contrary, $I{:}d_{(001)} > I{:}d_{(002)} > I{:}d_{(003)}$ holds in the triple chain length structure as revealed in the corresponding four polymorphs of SOS. The above relations were seen in POP, and in 1,2-dipalmitoyl-3-acyl-*sn*-glycerols (PPC_n); double for n = 12, 14, 16, and triple for n = 6, 8 (28).

In POP, α is double chain length, but γ, δ, β_2 and β_1 are triple chain length. The pseudo-β'_2 and pseudo-β'_1 forms are double chain length in contrast to pseudo-β' of SOS, because of the interlamellar distance of 42.4 A and also of the XRD intensity relation as described above. The small angle XRD proved that 42.4 A corresponds to $d_{(001)}$ (Fig. 2). Hence, one cannot read peak $d_{(003)}$ of $d_{(001)}$ = 129 A in a sextuple chain length structure (2,12). An alternative explanation is that 42.4 A is caused by an inclination of the triple chain against the lamella plane. The inclination angle can be estimated as 37 ± 1°, by assuming a length of one triple chain of POP, 70 ± 2 A [$d_{(002)}$ of 46.5 A for palmitoyl and 4 A for one glycerol, plus 20 ± 2 A for one oleoyl chain]. This angle of tilt is extraordinarily small, hence the triple chain length also is excluded.

Accordingly, we describe two pathways of the polymorphic transformation in POP in terms of the chain length structure as follows: double (α) → triple (γ) → double (pseudo-β'_2, pseudo-β'_1) → triple (β_2, β_1), and triple (δ) → double (pseudo-β'_1) → triple (β_2, β_1) which occurred only in the 99.2% sample. Similar conversions were reported in the past (Table 5); Malkin and Wilson (14): triple (β'' of long spacing, 68.5 A) → double (β' of 42.1 A) → triple (β of 60.7 A), Lavery (16): double (α of 47 A) → triple (β'' of 68 A) → double (β'-2 of 42.4 A) → triple (β-3 of 60.6 A), Lovegren et al. (26): double [5 of 16.05 A read as $d_{(003)}$] → triple [4, 3 of 37.4 A read as $d_{(002)}$] → double (2 of 44 A) → triple [1 of 31.5 A read as $d_{(002)}$], Gibon et al. (18):

double (α-2 of 50.1 A) → triple (L_2 or L_3 of 69.8 A) → double (sub-β'-2 of 45.1 A or pseudo-β'-2 of 43.8 A) → triple (β-3 of 61.6 A).

As seen here, the conversion from double to triple was observed in SOS and also in AOA and BOB (19), but the conversions like double-triple-double-triple were observed only in POP. The mechanistic consideration of this process will be given later.

Chain inclination. The chain inclination was assumed by calculating an increase of long spacing per two CH_2 units, Δl, through substitution of the saturated chains, as examined in 1,2-dioleoyl-3-acyl-*sn*-glycerol, OOC_n (31). Δl of the *trans* aliphatic chain normal to the basal surface is 2.54 A; hence, a chain inclination angle ω equals $\sin^{-1}(\Delta l/2.54)$. In the α form, Δl is 0.9 A obtained from the present study, and 1.3 A from the data on POP, SOS, AOA and BOB (19). This small increase is attributed mainly to disordered end packings due to intermingling saturated and oleoyl chains with different chain lengths. Therefore, we cannot calculate ω of α, yet it is likely that the chains in α are normal to the basal plane in analogy to α of mono-saturated acids TG.

In γ, $\Delta l = 2.55$ A (present) and 2.68 A (19), giving rise to $\omega \approx 90°$. Hence, the saturated chains are almost vertical to the basal plane. Accordingly, the oleoyl chains segregated from the saturated chains in the triple chain length structure, and glycerol bones might be arranged so that they enable the normal orientation of the saturated chains. The pseudo-β' form cannot be compared between POP and SOS, because of different chain length. Instead, the values of SOS, AOA and BOB of pseudo-β' (19) yield $\Delta l \sim 2.42$ A, and $\omega \sim 72°$. This value is a bit larger than 66° (2) or 67° (32) of β' in even-numbered mono-saturated TG. β_2 and β_1 have $\Delta l = 2.0$ A (present) and 2.1 A (19), giving rise to the inclination angles of 52° and 56°, respectively. Two values are far smaller than 63° (2) or 61° (32) of β in even-numbered mono-saturated acid TG. Instead, these values are very close to 55.8 of β of OOC_n, with even-numbered n = 14–24 (31). From the value of 55.8 in OOC_n, Kodali et al. assumed (31) that the saturated chain in β of OOC_n has nearly the same chain inclination angle as the oleoyl chain because the oleoyl chain in γ of oleic acid is 56.5 (33). The same consideration may be reasonable in β_2 and β_1 of SOS and POP.

Subcell structure. The α forms of POP and SOS are packed according to a hexagonal packing, because a single peak at 4.21 A was observed in the XRD short spacing. Hence, the zigzag planes of hydrocarbons are arranged in rotationally disordered orientation as in α of mono-acid TG (9,10). Interestingly, the value of 4.21 A is smaller than 4.36 A of triolein α (30), but larger than 4.14 A of tristearin α (34). Also, 4.21 A is comparable to 4.2 A of a gel phase of palmitoyl-oleoyl lecithin presumably packed in a hexagonal subcell (35), but larger than 4.11 A in a hexagonally-packed $P_{\beta'}$ phase of dipalmitoyl phosphatidylcholine (36). Coexistence of the saturated and oleoyl acyl chains within the same lamella may extend the lateral packing, due to steric hindrance of the *cis* double bond of the oleoyl chain.

In the triple chain-length structure, we must carefully interpret the results because data from polycrystalline samples must coincide with the lamella of saturated and oleoyl chains. Nevertheless, we can discuss the subcell structures to some extent, based on the XRD short spacing spectra. The subcell of γ is different from any other polymorphs of POP and SOS, because a peak of 4.74 A (POP) and 4.72 A (SOS) is unique (Fig. 1). The same result was obtained in AOA and BOB (19). This lattice parameter was observed only in γ of oleic acid having the $O'_{//}$ subcell (33,37). Accordingly, we predicted that the subcell structure similar to $O'_{//}$ would be revealed in γ. As for pseudo-β' of SOS, the lattice parameters are in a range of 3.7 and 4.3 A, having strong peaks at 4.02 and 3.70 A. This does not exclude a possibility that the stearoyl chain may be packed according to $O_\perp$ as in β_2', (4.2 and 3.8 A), or β'_1 (4.27, 4.13 and 3.79 A) of tristearin (20). Delta of POP, appearing in the 99.2% sample, also may be packed like pseudo-β' of SOS. The subcells of β_2 and β_1 resemble each other both in POP and SOS, because the two forms have very strong peaks at 4.61 A (POP) and 4.58 A (SOS) and weaker peaks around 3.6 ~ 3.9 A, which are characteristic of $T_{//}$ of mono-saturated acid TG (23,32). Therefore it is highly possible to assume $T_{//}$ in β_2 and β_1. Chapman observed the $T_{//}$ packing in the most stable form of SOS with infrared (38) and NMR techniques (39). Concerning subtle differences in the weaker peaks of the XRD short spacing between β_2 and β_1 (Fig. 1), it is worth noting that similar changes were detectable between β and α or γ of oleic acid (27). The most stable β form, being packed according to a $T_{//}$-like subcell (37), has a very strong peak at 3.68 A and a medium peak at 4.63 A. Hence, a simple superposition of the XRD short spacing patterns of β of tristearin and β of oleic acid results in the same pattern of β_1 of SOS. A similar trial using β of tristearin and α of oleic acid gave rise to the XRD short spacing pattern of β_2. In this regard, a model of SOS (23) that assumed $T_{//}$ in β of SOS and $O'_{//}$ in oleic acid for stearoyl and oleoyl lamella in the triple-layered structure, respectively, actually corresponds to β_2.

The pseudo-β'_2 and pseudo-β'_1 forms of POP may reveal complicated subcell packing, because the oleoyl and palmitoyl chains are packed in the same lamella. If the oleoyl chain retains an olefinic skew-*cis*-skew′ conformation as in γ of oleic acid (33,37), the single lamellae consisting of palmitoyl and oleoyl chains must be rather unstable due to serious steric hindrance (40). Nevertheless, the long spacing value of the two polymorphs, 42.4 A, is almost the same as that of β' of tripalmitin. Hence, we predict the oleoyl chain would reveal a specific olefinic conformation so that the chain-chain packing is stabilized. In this regard, one may note that there are a few olefinic conformations of one *cis* double bond besides skew-*cis*-skew′:skew-*cis*-skew-gauche in cholesteryl oleate at 123 K, giving rise to almost linear chain structure (41), skew-*cis*-skew in β of oleic acid (37), twisted skew-*cis*-skew′ resulting in the $O_\perp$ subcell in a low form of petroselinic acid, C_{18}:1, ω12 (42).

In addition to XRD, we examined powder Raman scattering spectra in a range of frequency 1400 ~ 1500 cm^{-1} concerning CH_2 scissoring mode. This mode is most sensitive to the packing arrangement of zigzag $-CH_2-$ planes (43). Figure 5 shows the data of γ, pseudo-β' and β_2 of SOS. From this we conclude that only pseudo-β' contains a perpendicular arrangement, whereas the other three are in the parallel packing, because a sharp band at 1416 cm^{-1}, denoted by an arrow in Figure 5, is detectable only in pseudo-β'. This band is indicative of the $O_\perp$

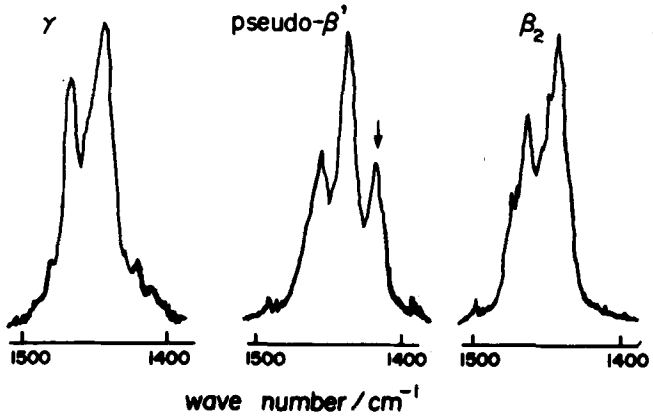

FIG. 5. Raman bands of CH_2 scissoring mode in γ, pseudo-β' and β_2 of SOS. The band denoted by an arrow is 1416 cm^{-1}.

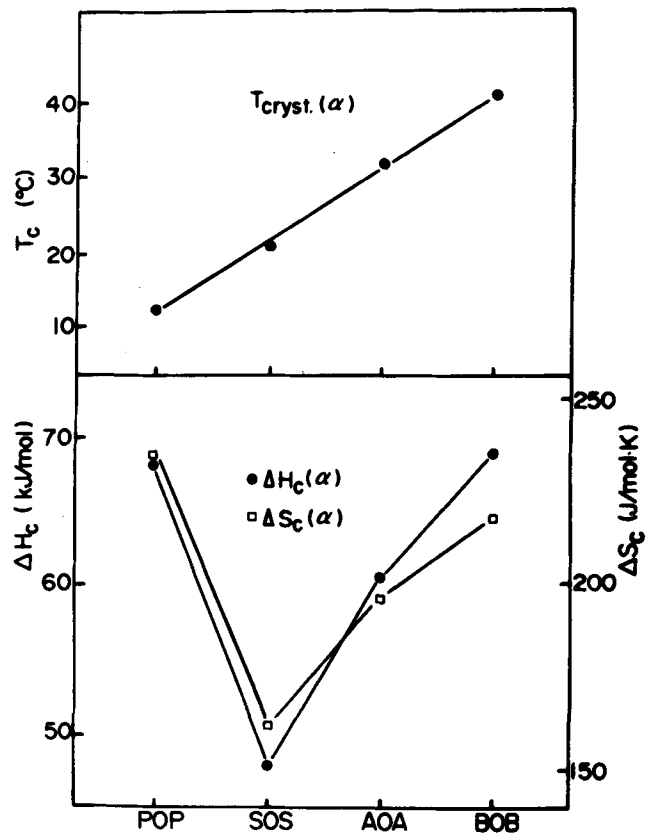

FIG. 6. Crystallization temperature (T_c), enthalpy (ΔH_c and entropy (ΔS_c) of melt crystallization of α in POP, SOS, AOA and BOB.

packing (43). This conclusion is consistent with the above consideration based on the XRD data. There was no appreciable difference between β_2 and β_1 in a wave number range of Figure 5. The Raman bands of pseudo-β'_2 and pseudo-β'_1 of POP differed from each other, and from pseudo-β' of SOS as well, indicating distinctive differences in the chain packing.

Thermal property. In view of the thermodynamic stability, a reasonable tendency was observed in Table 2, that T_m, ΔH_f and ΔS_f increased with increasing stability except for ΔH_f of δ of POP. The discrepancy with δ may be attributed to the difference in the chain length structure, namely δ is triple, but pseudo-β_2' and pseudo-β_1' are double.

As for ΔH_c of α, POP has an abnormally large value, e.g., $T_m(\alpha)$ of POP is lower than that of SOS by 8.3°C; conversely, $\Delta H_c(\alpha)$ of POP is larger than SOS by ca. 40%. This is contradictory to tripalmitin and tristearin, whose fusion parameters are always larger in tristearin with respect to every polymorph (3). To further clarify a peculiarity of POP α, crystallization temperature (T_c) and ΔH_c of melt crystallization were examined on AOA and BOB with DSC, as shown in Figure 6. T_c increased according to a linear dependence on the saturated acyl chain length over the four TGs. The same tendency was observed in ΔH_c in the case of SOS, AOA and BOB, but POP's value is much higher than that extrapolated from the linear dependency over the other three TGs. We interpret the results as follows. A total of lattice cohesive energy involves two major contributions: lateral chain-chain interaction and lamella-lamella interaction through CH_3 end packing. The bilayered α form contains disordered molecules in which steric hindrance between the saturated and oleoyl chains does not depend largely on the difference in the saturated acyl chain length. However, the CH_3 end packing may depend largely on the saturated acyl chain length. In the palmitoyl/oleoyl combination, better accommodation of the chain end packing due to similar chain length would be realized in comparison to other combinations.

The difference in ΔH_f between pseudo-β'_2 and β_2 and between pseudo-β'_1 and β_2 of POP are 28.9 kJ/mol and 26.1 kJ/mol, respectively. These values are a bit smaller than that between β' and β of tripalmitin, 31.8 kJ/mol (44). The ΔH_f difference between pseudo-β' and β_2 of SOS is 38.2 kJ/mol, which is also a bit smaller than that between β' and β of tristearin, 45.6 kJ/mol (44). As for β_2 and β_1, they differ in ΔH_f by 5.8 kJ/mol in POP and 8.0 kJ/mol in SOS. These are rather small, indicating subtle structural changes involved in the $\beta_2 \rightarrow \beta_1$ transformation. Both are smaller than ΔH = 8.8 kJ/mol of $\gamma \rightarrow \alpha$ transition in oleic acid which involves conformational disordering in the aliphatic chain between the double bond and the methyl end group (27,37).

ΔH_f of β_2 and β_1 of POP and SOS are all larger than $H_f(\beta)$ = 113.1 kJ/mol of triolein (45). ΔH_f of β_2 and β_1 of SOS are larger than ΔH_f = 132.9 kJ/mol of OSO (46). The two examples emphasize the importance of the saturated chain packing in β_2 and β_1. By dividing the ΔH_f differences between POP and SOS by the CH_2 difference, 4, we obtained ΔH_f/mol CH_2 4.65 kJ/mol for β_2 and 5.2 kJ/mol for β_1. Both are approximately comparable to ΔH_f/mol CH_2 in *trans* conformation for n-paraffin, 4 kJ/mol (47). For the β-form of tripalmitin (165.8 kJ/mol) and tristearin (191.8 kJ/mol), 4.3 kJ/mol was obtained by dividing the ΔH_f difference by six (48). This means that lattice cohesive energy contributed from the saturated chain is almost similar between POP and SOS for β_2 and β_1.

Polymorphic structure and phase transformation. It is rather difficult to decide the precise polymorphic structure based on the data obtained from the powder

sample. However, we tentatively depict four structure models, taking into account the structural and thermal properties obtained in the present study. One must note that the detailed conformations in the models, particularly of glycerol bone, olefinic and chain end groups are open to future study.

Figure 7a and 7b depicts two double chain length structures, in which the whole molecules are arranged vertically across the basal plane in (a), but inclined in (b). It is highly possible that the α form of POP and SOS may correspond to (a), and pseudo-β'_2 and pseudo-β'_1 of POP to (b). Two triple chain-length structures are possible. In Figure 7c, the saturated chains at the lamella interfaces are vertical across the basal plane, being connected to the glycerol bones and the oleoyl chains which are segregated into a single layer placed between the two glycerol bones. Meanwhile (Fig. 7d), the saturated chains are inclined with respect to the basal plane, and the segregated oleoyl chain is in a bent conformation like γ of oleic acid having the olefinic skew-*cis*-skew′ conformation. Due to connection with the glycerol bone, the directions of the oleoyl and saturated chains are approximately parallel. We infer that the γ form may correspond to Figure 7c and β_2 and β_1 to Figure 7d. In α, both the saturated and oleoyl chains are in less ordered conformation, as indicated by the Raman spectroscopy (M. Kobayashi, private communication). Broad XRD short spacing peaks around 4.4 ∼ 4.5 A in γ (Fig. 1 and Table 1) may correspond to the disordered conformation in the oleoyl lamellae. The pseudo-β' form of SOS may also form Figure 7d, although the chain inclination is less enhanced than β_2.

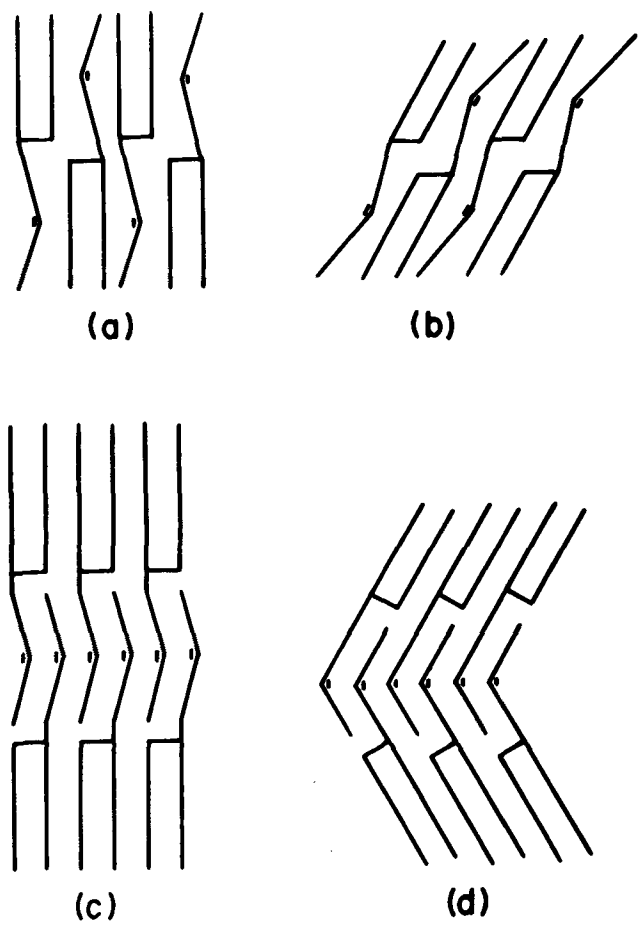

FIG. 7. Postulated structure models of double chain length, (a) and (b), and triple chain length, (c) and (d), of the polymorphs of POP and SOS.

The polymorphic transformation may be discussed based on the postulated structure models. Melt chilling produces α, in which disordered molecular conformations form the bilayered structure as illustrated in Figure 7a. Upon stabilization, the chain segregation first occurs through the $\alpha \rightarrow \gamma$ transformation, keeping rather loose packing both in the saturated and oleoyl chains. After $\alpha \rightarrow \gamma$, the stabilization may be determined by equilibration between the lamella-lamlella end group packing and the lateral chain-chain packing. The end packing is less stabilized in the TG having the acyl chains with largely different chain lengths due to interpenetrating lamella structure. The chain-chain packing is most disturbed by a joint packing of *cis* double bond and *trans* saturated chain. It is likely that the first stabilization might let γ of POP transform into the bilayered pseudo-β'_2 in which the unstabilized interaction between oleoyl and palmitoyl chains may be compensated for by the stabilized end packing. Obviously, the situation for occurrence of the two pseudo-β' forms of POP must be marginal, as the impurity subtly caused an occurrence of triple-layered δ form. Chain slip movement accompanied with the transformations of triple-layered $\gamma \rightarrow$ double-layered pseudo-β'_2 may be allowed due to loose packing in the γ form. In the case of SOS, γ does not transform to the bilayered structure due to unstable end packing, but converts to pseudo-β' keeping the triple chain length structure. It is still uncertain why the same process as SOS did not occur in POP. We infer that the organization of $O_\perp$ packing, as observed in pseudo-β' of SOS, from the γ form may also encounter steric hindrance. Upon further stabilization from the pseudo-β' forms, no coexistence of the saturated and oleoyl chains is allowed, so that the chain segregation may occur even in POP. In a final conversion from β_2 to β_1, it appears that changes would be revealed primarily in the oleoyl chain and the glycerol bone, keeping the interlamella distance constant.

Nonsynchronous conversion among the DSC melting peak and the XRD short and long spacing spectra (Table 4) may be related to characteristic structural changes involved in the phase transformation. The general tendency that the initiation and completion of transformation were most manifest in the short spacing may be due to the smallest resistance in the chain packing rearrangement. It appears that the transformation involving a conversion in the chain length structure occurred in a nonsynchronous way among the three indicators. In the particular case of pseudo-$\beta'_2 \rightarrow \beta_2$ in POP involving the double → triple conversion, the long spacing was completed extraordinarily slowly. It is still not possible to explain this process. Further study using the data more sensitive to the lamella-lamella interaction like infrared spectra must be done.

To conclude, the present examination gave rise to five and six independent polymorphs in SOS and POP, respectively. The molecular structures and mechanistic consideration were presented to explain rather complicated polymorpic behavior. Further studies to obtain more

precise knowledge of the molecular structures using single crystals are needed. In addition, to relate the present study to problems in confectionery fat, the β_2 and β_1 forms may correspond to Form V and Form VI of cocoa butter (49), respectively, according to quite similar polymorphic behavior (21). A variety of mixtures of POP/POS/SOS supported this conclusion (50), in contrast to an interpretation which does not regard Form V and Form VI as independent polymorphs (51). Therefore, the present findings will be useful to elucidate the polymorphic behavior of cocoa butter.

ACKNOWLEDGMENT

The authors are indebted to M. Kobayashi, Osaka University, for unpublished data of Raman study and valuable discussion.

REFERENCES

1. *Bailey's Industrial Oil and Fat Products, Vol. 1,* 4th edn., edited by D. Swern, John Wiley & Sons, New York, 1979, p. 177.
2. Small, D.M., in *Handbook of Lipid Research, Vol. 4,* edited by D.J. Hanahan, Plenum, New York, 1986, p. 345.
3. Hagemann, J.W., in *Crystallization and Polymorphism of Fats and Fatty Acids,* edited by N. Garti and K. Sato, Marcel Dekker, New York, 1988, p. 9.
4. Jensen, L.H., and A.J. Mabis, *Acta Crystallogr. 21*:770 (1966).
5. Larsson, K., *Arkiv Kemi 23*:1 (1964).
6. De Jong, S., and T.C. van Soest, *Ibid. B34*: 1570 (1978).
7. Precht, D., and E. Frede, *Ibid. B39*:381 (1983).
8. Hernqvist, L., and K. Larsson, *Fette, Seifen, Anstrichm. 84*: 349 (1982).
9. Larsson, K., *Arkiv Kemi 23*:35 (1965).
10. Hagemann, J.W., and J.A. Rothfus, *J. Am. Oil Chem. Soc. 60*:1308 (1983).
11. Daubert, B.F., and T.H. Clarke, *J. Am. Chem. Soc. 66*:690 (1944).
12. Filer, L.J., S.S. Sidhu, B.F. Daubert and H.E. Longenecker, *J. Am. Chem. Soc. 68*:167 (1946).
13. Lutton, E.S., *J. Am. Chem. Soc. 68*:676 (1946).
14. Malkin, T., and B.R. Wilson, *J. Chem. Soc.* 369 (1949).
15. Lutton, E.S., and F.L. Jackson, *J. Am. Chem. Soc. 72*:3254 (1950).
16. Lavery, H., *J. Am. Oil Chem. Soc. 35*:418 (1958).
17. Landmann, W., R.O. Feuge and N.V. Lovegren, *Ibid. 37*:638 (1960).
18. Gibon, V., F. Durant and Cl. Deroanne, *Ibid. 63*:1047 (1986).
19. Wang, Z.H., K. Sato, N. Sagi, T. Izumi and H. Mori, *J. Jpn. Oil Chem. Soc. 36*:671 (1987).
20. Simpson, T.D., and J.W. Hagemann, *J. Am. Oil Chem. Soc. 59*:169 (1982).
21. Sato, K., *Food Microstructure 6*:151 (1987).
22. Sato, K., and T. Kuroda, *J. Am. Oil Chem. Soc. 64*:124 (1987).
23. Larsson, K., *Fette, Seifen, Anstrichm. 74*:136 (1972).
24. Larsson, K., *Acta Chem. Scand. 20*:2255 (1966).
25. Hernqvist, L., B. Herslof and M. Herslof, *Fette, Seifen, Anstrichm. 86*:393 (1984).
26. Lovegren, N.V., M.S. Gray and R.O. Feuge, *J. Am. Oil Chem. Soc. 48*:116 (1971).
27. Suzuki, M., T. Ogaki and K. Sato, *Ibid. 62*:1600 (1985); Erratum, *J. Am. Oil Chem. Soc. 63*:553 (1986).
28. Kodali, D., D. Atkinson, T.G. Redgrave and D.M. Small, *Ibid. 61*:1078 (1984).
29. Lutton, E.S., *J. Am. Chem. Soc. 67*:524 (1945).
30. Ferguson, R.H., and E.S. Lutton, *Ibid. 69*:1445 (1947).
31. Fahey, D.A., D.M. Small, D. Kodali, D. Atkinson and T.G. Redgrave, *Biochemistry 24*:3757 (1985).
32. Malkin, T., *Prog. Chem. Fats Other Lipids,* Vol. 2, Pergamon Press, London, 1954, p. 1.
33. Abrahamsson, S., and I. Ryderstadt-Nahringbauer, *Acta Crystallogr. 15*:1261 (1962).
34. Dafler, J.R., *J. Am. Oil Chem. Soc. 54*:250 (1977).
35. Coolber, K.P., C.B. Berde and K.M.W. Keough, *Biochemistry 22*:1466 (1983).
36. Ruocco, M.J., and G.G. Shipley, *Biochim. Biophys. Acta 684*:59 (1982).
37. Kobayashi, M., F. Kaneko, K. Sato and M. Suzuki, *J. Phys. Chem. 90*:6371 (1986).
38. Chapman, D., *J. Am. Oil Chem. Soc. 37*:73 (1960).
39. Chapman, D., R.E. Richards and R.W. Yorke, *J. Chem. Soc.* 436 (1960).
40. Small, D.M., *J. Lipid Res. 25*:1490 (1984).
41. Gao, Q., and B.M. Craven, *Ibid. 27*:1214 (1986).
42. Kaneko, F., M. Kobayashi, K. Sato, M. Suzuki, Y. Kitagawa and Y. Matsuura, in *Collected Abstracts of ISF-JOCS World Congress,* Tokyo, 1988, p. 210.
43. Kobayashi, M., in *Crystallization and Polymorphism of Fats and Fatty Acids,* edited by N. Garti and K. Sato, Marcel Dekker Inc., New York, 1988, p. 139.
44. Ollivon, M., and R. Perron, *Thermochim. Acta 53*:183 (1982).
45. Timms, R.E., *Chem. Phys. Lipids 21*:113 (1978).
46. Kodali, D.R., D. Atkinson, T.G. Redgrave and D.M. Small, *J. Lipid Res. 28*:403 (1987).
47. Small, D.M., in *Handbook of Lipid Research,* Vol. 4, edited by D.J. Hanahan, Plenum, New York, 1986, p. 183.
48. Hagemann, J.W., and J.A. Rothfus, *J. Am. Oil Chem. Soc. 60*:1123 (1983).
49. Wille, R.L., and E.S. Lutton, *Ibid. 43*:491 (1966).
50. Sagi, N., T. Arishima, H. Mori and K. Sato, *J. Jpn. Oil Chem. Soc.,* in press.
51. Hernqvist, L., in *Industrial Chocolate Manufacturing and Use,* edited by S.T. Beckett, Blackie, Glasgow, Scotland, 1988, p. 159.

[Received August 5, 1988; accepted December 17, 1988]
[J5540]